Observation of high-j quasiparticle states in ^{249}Cm by in-beam γ-ray spectroscopy using heavy-ion transfer reactions

T. Ishii,[1,2,*] H. Makii,[3] M. Asai,[2] K. Tsukada,[2] A. Toyoshima,[2] M. Matsuda,[1] A. Makishima,[4] S. Shigematsu,[5] J. Kaneko,[6] T. Shizuma,[7] H. Toume,[2,8] I. Hossain,[9,†] T. Kohno,[5] and M. Ogawa[6]

[1]*Department of Research Reactor and Tandem Accelerator, Japan Atomic Energy Agency, Tokai, Ibaraki 319-1195, Japan*
[2]*Advanced Science Research Center, Japan Atomic Energy Agency, Tokai, Ibaraki 319-1195, Japan*
[3]*Institute of Particle and Nuclear Studies, High Energy Accelerator Research Organization (KEK), Tokai, Ibaraki 319-1195, Japan*
[4]*Department of Liberal Arts and Sciences, National Defense Medical College, Tokorozawa, Saitama 359-8513, Japan*
[5]*Department of Energy Sciences, Tokyo Institute of Technology, Yokohama 226-8502, Japan*
[6]*Department of Radiological Sciences, Komazawa University, Setagaya, Tokyo 154-8525, Japan*
[7]*Quantum Beam Science Directorate, Japan Atomic Energy Agency, Kyoto 619-0215, Japan*
[8]*College of Science, Ibaraki University, Mito, Ibaraki 310-8512, Japan*
[9]*Department of Physics, Osaka University, Toyonaka, Osaka 560-0043, Japan*

We have measured de-excitation γ rays in ^{249}Cm populated by one-neutron stripping reactions with a ^{248}Cm target and 162-MeV ^{16}O, 162-MeV ^{18}O, and 120-MeV ^{13}C beams. γ rays in ^{249}Cm were identified by measuring kinetic energies of outgoing particles using Si ΔE-E detectors. It was demonstrated that high-j orbitals were selectively populated in the (^{16}O, ^{15}O) reaction having a large negative Q value. We have observed eight quasiparticle states above the deformed shell gap of $N = 152$. The $1/2^+$[620], $1/2^-$[750], and $7/2^+$[613] bands were extended up to $19/2^+$, $19/2^-$, and $13/2^+$ states, respectively. We have established the $9/2$ $9/2^+$[615] state at 526 keV, the $9/2$ $9/2^+$[604] state with a short life of $T_{1/2} \ll 2$ ps at 1030 keV, and the $11/2$ $11/2^-$[725] state with $T_{1/2} = 19(1)$ ns at 375 keV. Furthermore, the $17/2$ $1/2^+$[880] state, having a large component of the $k_{17/2}$ spherical single-particle state, has been identified at 1505 keV. We discuss the properties of those quasiparticle states in the framework of a deformed shell model.

DOI: 10.1103/PhysRevC.78.054309   PACS number(s): 23.20.−g, 21.60.Ev, 25.70.Hi, 27.90.+b

I. INTRODUCTION

High-j single-particle states play an important role in nuclear structure of superheavy nuclei because of their large angular momenta and their large degeneracy. Neutron(ν) $j_{13/2}$ and $k_{17/2}$ and proton (π) $i_{11/2}$ and $j_{15/2}$ orbitals lie above possible spherical shell gaps of $N = 184$ and $Z = 114$. In heavy-actinide deformed nuclei, quasiparticle states having a large component of those spherical single-particle states may be observed, because the $K = 1/2$ quasiparticle states originating from those spherical states become very low in energy at prolate deformation. Until now, quasiparticle states of $1/2^-$[521] and $1/2^-$[750], having a large component of $\pi f_{5/2}$ above $Z = 114$ and $\nu h_{11/2}$ above $N = 184$, respectively, were identified [1,2]. Quasiparticle states of $1/2^-$[761] and $1/2^+$[880], having a high-j component of $\nu j_{13/2}$ and $\nu k_{17/2}$, were reported [3,4], but these states are still uncertain. In the present experiment, we intended to identify high-j orbitals in ^{249}Cm.

Recently, nuclear structure study of heavy-actinide nuclei progressed by in-beam γ-ray and electron spectroscopy and isomer-decay spectroscopy using recoil decay tagging techniques [5–8]. Because those heavy-actinide nuclei were produced by heavy-ion fusion reactions, it is difficult to approach nuclei with a large neutron number. $N = 153$ is a frontier of the largest neutron number in which quasiparticle states were studied experimentally. Low-spin states in ^{253}Fm$_{153}$ were identified by α-γ and α-electron spectroscopy of ^{257}No [9]. Quasiparticle states in ^{251}Cf$_{153}$ have been investigated intensively; eight quasiparticle states above the $N = 152$ deformed shell gap were identified by α-decay spectroscopy of ^{255}Fm [10–13], EC-decay spectroscopy of ^{251}Es [13], and (d, p) transfer reaction study using a highly radioactive target of ^{250}Cf [3]. Quasiparticle states in ^{249}Cm$_{153}$ were studied by α-decay spectroscopy of ^{253}Cf [14], (d, p) transfer reaction study [15], and (n, γ) spectroscopy [16]. Furthermore, high-j states in ^{249}Cm were studied by the (^{4}He,^{3}He) transfer reaction [4]. Quasiparticle states in ^{249}Cm, however, were less established than those in ^{251}Cf.

We have developed a spectroscopic method of combining particle and γ-ray measurements using heavy-ion transfer reactions [17]. This method was applied to measuring in-beam γ rays in neutron-rich actinide nuclei of ^{236}Th, ^{240,242}U, ^{246}Pu, and ^{250}Cm using the (^{18}O,^{16}O) and (^{18}O,^{20}Ne) two-nucleon transfer reactions [17–20]. In the present study, we have used the one neutron-stripping reaction of (^{16}O, ^{15}O) having a large negative Q value to observe high-j quasiparticle states in ^{249}Cm. This transfer reaction populates levels with high angular momentum because of matching condition. Bond *et al.* [21] showed that the (^{16}O, ^{15}O) reaction populates high-j orbitals in Er nuclei by measuring γ-rays in coincidence with outgoing particles using a Q3D spectrometer. We have used Si ΔE-E detectors for selecting outgoing particles and

---

*ishii.tetsuro@jaea.go.jp
†On leave from Department of Physics, Shah Jalal University of Science and Technology, Sylhet 3114, Bangladesh.

measuring their kinetic energies. Although the present setup gives a poor energy resolution for a reaction Q value owing to kinematic broadening, the Si detectors cover much larger solid angles than the magnetic spectrometer. This merit made it possible to make a full-fledged γ-ray spectroscopy such as particle-γ-γ coincidence. We have also carried out in-beam γ-ray experiments using the (^{18}O, ^{17}O) and (^{13}C, ^{12}C) reactions so as to clarify the properties of the (^{16}O, ^{15}O) reaction and to distinguish high-j orbitals.

We have observed eight quasiparticle states in ^{249}Cm, including a $1/2^+$[880] state originating from the $k_{17/2}$ orbital. We discuss the properties of those quasiparticle states in the framework of a deformed shell model, using parameters derived by a comprehensive survey of the actinide region [2]. The excitation energy of the $17/2$ $1/2^+$[880] state was identified to be 1505 keV, which is close in energy to one of the candidates observed in the (^{4}He,^{3}He) transfer reaction [4]. This low excitation energy of the $17/2$ $1/2^+$[880] state was predicted by a calculation using a momentum-dependent Woods-Saxon potential [3].

II. EXPERIMENTS

The experiments were carried out at the JAEA-Tokai tandem accelerator facility [22]. We used a ^{248}Cm target, with 0.8 mg/cm^2 thickness and 3 mm diameter, electrodeposited on a 3-μm aluminum foil. The isotopic compositions of the Cm target were 96.7, 0.04, 3.1, 0.15, and 0.007% for the mass numbers of 248, 247, 246, 245, and 244, respectively. The total radioactivity of the target was 45 kBq; ^{244}Cm, with a short lifetime of $T_{1/2} = 18.1$ years, contributes to this radioactivity at the same level as that of ^{248}Cm in spite of its low concentration. The target was bombarded by a 162-MeV ^{16}O beam with 0.3 particle nA, a 162-MeV ^{18}O beam with 0.3 particle nA, and a 120-MeV ^{13}C beam with 0.3 particle nA. The total doses were 5.9×10^{14} ions of ^{16}O, 5.9×10^{14} ions of ^{18}O, and 3.3×10^{14} ions of ^{13}C. The beams were adjusted so as not to hit a collimator of 2.5 mm in diameter placed in front of the target. Residual nuclei produced by the transfer reaction stop in the aluminum backing. Most in-beam γ rays in residual nuclei were measured without Doppler shifts, because most excited states populated by the transfer reactions have lifetimes longer than the stopping time of approximately 2 ps.

Schematic view of experimental setup is shown in Fig. 1. Outgoing nuclei were detected using four sets of Si ΔE-E detectors of 20 mm in diameter, and γ rays emitted from residual nuclei were measured using six Ge detectors in coincidence with the outgoing nuclei. These four Si ΔE-E detectors were placed at $40°$ with respect to the beam axis, at a distance of 5 cm from the target. The Si ΔE detectors were surface-barrier type of 75 μm in thickness made by ourselves from an ELID (*el*ectrolytic *i*n-process *d*ressing)-grinding Si wafer supplied by NEXSYS Corp. The uniformity of the thickness of this wafer, which dominates the resolution of the ΔE detector, was achieved within ± 1 μm. In heavy-ion transfer reactions, outgoing particles have a bell-shaped angular distribution near the grazing angle, providing that the range of angular momenta contributing to nucleon transfer is not too narrow [23]. By the DWBA calculation using PTOLEMY
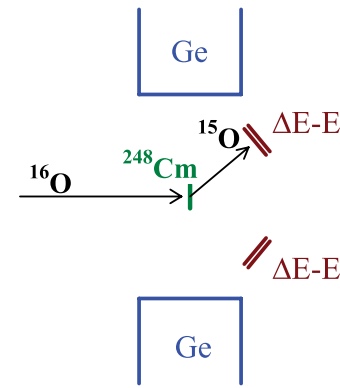

FIG. 1. (Color online) Schematic view of experimental setup drawn in section horizontally (vertically). Four sets of Si ΔE-E detectors were placed at $40°$ with respect to the beam axis. These four Si detectors and four Ge detectors were placed symmetrically; two of them were placed in the horizontal plane, and the other two were placed in the vertical plane. Two more Ge detectors (not depicted here) were also placed between the former Ge detectors.

code [24], the cross sections of the (^{16}O, ^{15}O), (^{18}O, ^{17}O), and (^{13}C, ^{12}C) reactions have bell shapes with a peak around $40°$ in the laboratory frame at the incident energies employed in the experiment. The detection efficiencies for these particles were estimated as 36%, by considering the solid angles of the Si detectors and the particle angular distributions calculated with PTOLEMY.

Four of the six Ge detectors, with 60% relative efficiency, were arranged symmetrically in the plane perpendicular to the beam axis at a distance of 6 cm from the target. Two of the Ge detectors and two of the Si ΔE-E detectors were placed in the vertical plane including the beam axis, and the other two Ge detectors and two Si detectors were placed in the horizontal plane. This setup allows one to measure the anisotropies of γ rays emitted in the reaction plane to those out of the reaction plane. The remaining two Ge detectors, with 30% relative efficiency, were placed between the former Ge detectors. The absolute efficiencies of the total Ge detectors were 12 and 3.0% for 0.20 and 1.33 MeV, respectively. We recorded the particle-γ-(γ)-t coincidence data. The time differences between the particle and γ-ray signals were measured using TACs (time to amplitude converters).

III. RESULTS

An E-ΔE plot obtained from the experiment using the ^{16}O beam is shown in Fig. 2. Outgoing nuclei were separated not only by atomic number but also by mass number. The energy signals of ΔE and E detectors were calibrated using the peak of elastically scattered particles. The dashed line in Fig. 2 represents a calculated energy loss for ^{15}O particles. The ^{15}O particle has a maximum kinetic energy when the ^{15}O and ^{249}Cm nuclei lie at the ground state. In this ground-state reaction, the incident energy of ^{15}O onto the Si detector is 143 MeV, when the ^{15}O nucleus is scattered at the center of the Si detector. The decrement in the kinetic energy of ^{15}O corresponds to the excitation energy of ^{249}Cm when the ^{15}O nucleus is not excited. This is valid at least below 5.18 MeV,
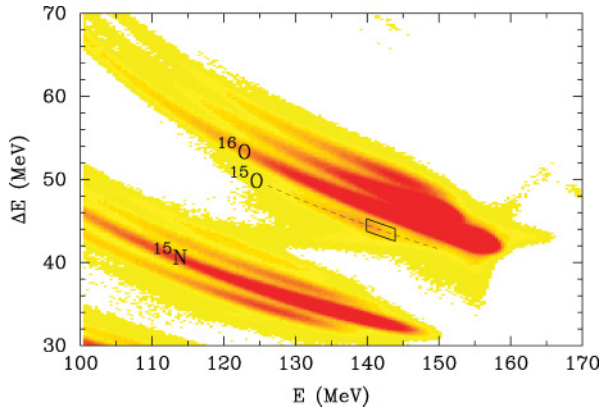
FIG. 2. (Color online) E-ΔE plot of scattered particles measured by a Si ΔE-E detector in the reaction of a 162-MeV ^{16}O beam with a ^{248}Cm target. The dashed line represents a calculated energy loss for ^{15}O nuclei. The enclosed area with solid lines corresponds to the excitation energy of ^{249}Cm between -1 and 3 MeV.

the first excitation energy of ^{15}O. The ^{15}O kinetic energies indicated by the enclosed area with solid lines in Fig. 2 correspond to the excitation energies E_x of ^{249}Cm between -1 and 3 MeV. This area was used as the gate for the analysis of the ^{15}O-γ coincidence. Note that the kinematic broadening due to the solid angles subtended by the Si detector is approximately 2 MeV.

Figures 3, 4, and 5 show γ-ray spectra of ^{249}Cm. Figure 3(a) was obtained in the (^{16}O, ^{15}O) reaction by setting the gates of ^{15}O whose kinetic energies correspond to E_x of ^{249}Cm between -1 and 3 MeV, as shown in Fig. 2. Figures 3(b) and 3(c) were measured in the (^{18}O, ^{17}O) and (^{13}C, ^{12}C) reactions by setting the gates of ^{17}O and ^{12}C, respectively, corresponding to E_x between -1 and 3 MeV. Figures 4 and 5 are the same as Fig. 3, but for the γ-ray energy range. As shown in these figures, γ-ray spectra of ^{249}Cm observed in the (^{16}O, ^{15}O) reaction are very different from those in (^{13}C, ^{12}C). γ rays in ^{249}Cm are summarized in Table I. In this table, γ-ray intensities represent γ-ray emission yields in the units of μb, and total internal conversion coefficients α_T were taken from Ref. [25].

Figure 6 shows γ-ray spectrum obtained by the ^{16}O gate in the (^{18}O, ^{16}O) reaction. The kinetic energies of ^{16}O were selected as corresponding to the excitation energy of ^{250}Cm between 9 and 12 MeV. Because neutron separation energy of ^{250}Cm is 5.8 MeV, ^{249}Cm is produced by one neutron evaporation. γ rays in ^{249}Cm observed in this reaction are emitted from near the yrast line, because these γ rays follow successive decay from higher excited states. This γ-ray spectrum has high continuum background, which would come from prompt γ rays of fission products [26].

Nuclei produced by heavy-ion transfer reactions are polarized perpendicular to the reaction plane defined by the beam axis and a Si ΔE-E detector. Therefore, γ rays emitted from these nuclei show in-plane to out-of-plane anisotropies depending on the types of transitions. For stretched dipole and quadrupole transitions, angular distributions $W(\theta)$ are proportional to $1 + \cos^2(\theta)$ and $1 - \cos^4(\theta)$, respectively, where θ is the angle measured from the polarization axis.
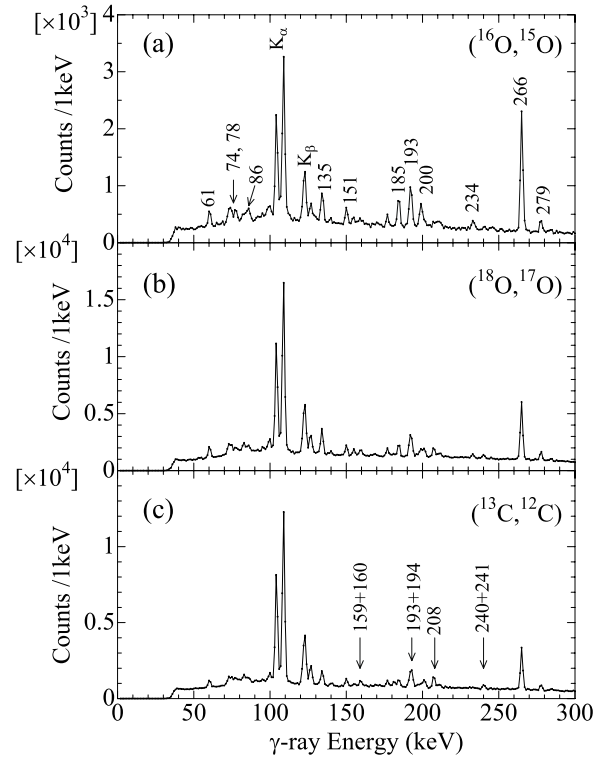

FIG. 3. γ-ray spectra of ^{249}Cm. The spectrum (a) was measured in the reaction of (^{16}O, ^{15}O) by setting the gate on ^{15}O with kinetic energies indicated by the enclosed area in Fig. 2. The spectra (b) and (c) were measured in the reaction of (^{18}O, ^{17}O) and (^{13}C, ^{12}C), respectively, by setting the gates on ^{17}O and ^{12}C whose kinetic energies are selected so that the excitation energy ranges of ^{249}Cm become the same as the ^{15}O gate ($-1 < E_x < 3$ MeV). γ rays in ^{249}Cm are labeled in the spectra; labeled in the spectrum (c) are γ peaks observed clearer in (^{13}C, ^{12}C) than in (^{16}O, ^{15}O).

Thus, γ-ray anisotropies were obtained as $I_{\gamma\text{in}}/I_{\gamma\text{out}} > 1$ for a stretched quadrupole transition and <1 for a stretched dipole transition. For not stretched or mixed transitions, see Ref. [27]. In-plane to out-of-plane ratios were obtained using four Si ΔE-E detectors and four Ge detectors placed symmetrically. In-plane and out-of-plane intensities, $I_{\gamma\text{in}}$ and $I_{\gamma\text{out}}$, were obtained from $I_{\gamma\text{in}} = \sum_{i=1}^{4}[I_\gamma(s_i g_i) + I_\gamma(s_i g_{i+2})]$, and $I_{\gamma\text{out}} = \sum_{i=1}^{4}[I_\gamma(s_i g_{i+1}) + I_\gamma(s_i g_{i+3})]$, where s_i, g_i denote the i-th Si and Ge detectors adjacent to each other and $I(s_i g_j)$ denotes the γ-ray counts measured by the combination of s_i and g_j (if $j > 4$, j is replaced with $j - 4$). In this analysis, the detection efficiencies for $I_{\gamma\text{in}}$ and $I_{\gamma\text{out}}$ are $\epsilon_{\text{in}} = \sum_{i=1}^{4}[\epsilon(s_i)\epsilon(g_i) + \epsilon(s_i)\epsilon(g_{i+2})]$, and $\epsilon_{\text{out}} = \sum_{i=1}^{4}[\epsilon(s_i)\epsilon(g_{i+1}) + \epsilon(s_i)\epsilon(g_{i+3})]$, respectively. Therefore, $\epsilon_{\text{in}} = \epsilon_{\text{out}}$, if $\epsilon(s_1) + \epsilon(s_3) = \epsilon(s_2) + \epsilon(s_4)$ or $\epsilon(g_1) + \epsilon(g_3) = \epsilon(g_2) + \epsilon(g_4)$. Because the Si and Ge detectors were placed almost symmetrically in the present experiment, ϵ_{in} is expected to be equal to ϵ_{out}. In fact, $I_{\gamma\text{in}}/I_{\gamma\text{out}}$ was unity for K x rays. Anisotropies $I_{\gamma\text{in}}/I_{\gamma\text{out}}$ are listed in Table I; most data were taken from the (^{16}O, ^{15}O) experiment, and some data were from the (^{13}C, ^{12}C) experiment. Anisotropy results give information on the multipolarity of γ transitions. Detailed discussion will be given in the following section.

TABLE I. γ-ray energies, intensities, and in-pane to out-of-plane intensity ratios of ^{249}Cm.

$I_i \to I_f$	E_γ (keV)	I_γ (μb)	$I_\gamma(1+\alpha_T)$ (μb)				$I_{\gamma_{in}}/I_{\gamma_{out}}$
		(^{16}O, ^{15}O)	(^{16}O, ^{15}O)	(^{18}O, ^{17}O)	(^{13}C, ^{12}C)	(^{18}O, ^{16}On)	(^{16}O, ^{15}O)
$1/2^+$[620]							
$11/2^+ \to 7/2^+$	134.6(1)	18.0(13)	109(8)	420(20)	350(20)	88(11)	2.3(3)
$15/2^+ \to 11/2^+$	185.0(1)	20.5(15)	49(4)	103(7)	97(8)	55(5)	2.2(3)
$19/2^+ \to 15/2^+$	233.7(1)	9.5(11)	15(2)	30(4)	17(5)	35(4)	1.9(5)
$13/2^+ \to 9/2^+$	150.6(1)	9.6(10)	40(4)	119(9)	118(11)	52(9)	1.3(3)
$17/2^+ \to 13/2^+$	199.6(2)	22.7(17)	46(3)	116(8)	107(9)	45(5)	1.7(2)
$1/2^-$[750] $\to 1/2^+$[620]							
$1/2^- \to 1/2^+$	494.3(2)	<0.7		19(3)	60(5)		1.1(2)[a]
$1/2^- \to 3/2^+$	468.1(3)	<0.8		14(4)	46(13)		0.89(9)[a]
$3/2^- \to 1/2^+$	470.1(2)	3.2(13)	3(1)	24(6)	60(20)		0.89(9)[a]
$3/2^- \to 5/2^+$	422.0(1)	<4		49(4)	138(8)		0.80(6)[a]
$7/2^- \to 5/2^+$	453.8(1)	8.3(11)	9(1)	116(6)	161(9)		0.75(5)[a]
$7/2^- \to 9/2^+$	353.6(1)	7.7(11)	8(1)	96(6)	138(8)		0.92(6)[a]
$11/2^- \to 9/2^+$	429.1(1)	32.3(22)	33(2)	113(6)	101(6)		0.63(6)
$11/2^- \to 13/2^+$	278.5(1)	11.7(12)	12(1)	42(3)	38(4)		0.8(2)
$15/2^- \to 13/2^+$	400.1(1)	21.1(17)	22(2)	52(4)	41(4)	15(2)	0.66(9)
$19/2^- \to 17/2^+$	369.7(1)	14.5(14)	15(2)	19(3)	<15	21(3)	0.68(13)
$1/2^+$[880] $\to 1/2^-$[750]							
$17/2^+ \to 19/2^-$	636.5(5)	9.8(16)	10(2)	<3	<4		1.1(4)
$3/2^+$[622] $\to 1/2^+$[620], $7/2^+$[613]							
$3/2^+ \to 1/2^+$	208.0(1)	4.5(9)	23(5)	186(14)	280(20)		1.3(2)[a]
$3/2^+ \to 5/2^+, 7/2^+$	159.9(2)	5.6(10)	37(7)	150(20)	190(20)		0.7(2)[a]
$5/2^+ \to 5/2^+, 7/2^+$	193.5(3)						
$7/2^+ \to 5/2^+, 7/2^+$	240.6(1)	3.4(12)	13(4)	73(10)	100(14)		0.8(2)[a]
$7/2^+$[613]							
$9/2^+ \to 7/2^+$	60.8(1)	11.2(11)	370(40)	1210(90)	1100(100)		0.43(9)
$11/2^+ \to 9/2^+$	73.6(3)	16.5(14)	320(30)	<1200	<1200		0.77(12)
$13/2^+ \to 11/2^+$	86.0(2)	9.3(10)	117(13)	<350	<380		0.65(14)
$9/2^+$[615] $\to 7/2^+$[613]							
$9/2^+ \to 7/2^+$	477.6(1)	13.6(14)	14(1)	85(5)	82(6)		0.9(2)
$9/2^+ \to 9/2^+$	417.0(1)	10.7(12)	11(1)	52(4)	50(4)		2.6(7)
$9/2^+$[604] $\to 7/2^+$[613]							
$9/2^+ \to 7/2^+$	981.1(5)	23.1(26)	25(3)	120(9)	122(11)		0.50(14)
$11/2^-$[725] $\to 7/2^+$[613]							
$11/2^- \to 9/2^+$	265.7(1)	108(6)	114(6)	271(14)	261(14)	91(5)	0.99(4)
$11/2^- \to 11/2^+$	192.5(1)	34.9(22)[b]	39(2)[b]	115(6)[b]	130(8)[b]	43(4)[b]	0.99(8)
K x rays and other γ rays							
	K_α	171(9)	171(9)	830(40)	1100(60)		0.94(3)
	K_β	50(3)	50(3)	240(12)	320(20)		1.08(8)
	77.8(2)	9.5(10)	156(17)	<470	<610		0.59(13)
	441.5(1)	<3.1		20(3)	42(4)		0.8(2)[a]
	524.4(2)	2.1(10)	2.2(10)	39(4)	93(10)		
	526.1(2)	6.7(14)	6.8(14)	75(6)	64(9)		0.65(5)[a]

[a]The ratio was obtained from the intensities measured in the (^{13}C, ^{12}C) reaction.
[b]The value contains intensities of the 193.5-keV transitions ($3/2^+$[622] $\to 1/2^+$[620], $7/2^+$[613]).

γ-γ coincidence relationships are summarized in Table II. Some γ-γ coincidence spectra measured in the (^{16}O, ^{15}O) reaction are shown in Figs. 7(a)–7(c). In this analysis, the gates for ^{15}O were set in the kinetic energies corresponding to E_x between -1 and 5 MeV. γ-γ coincidence relations under the delayed condition (^{15}O-γ coincidence time between 20 and 100 ns) were also analyzed for confirming the decay of the 375-keV level.

We established a level scheme as shown in Fig. 8. We constructed this level scheme on the basis of γ-ray energies, intensities, anisotropies, and γ-γ coincidence relationships, consulting the result of the (d, p) transfer reaction experiment [15]. In this level scheme, transitions observed in the (^{16}O, ^{15}O) reaction are depicted.

Figures 9(a) and 9(b) show decay curves for the transitions de-exciting the 375-keV level. These decay curves were

TABLE II. γ-γ coincidence relationships observed in ^{249}Cm.

Gate	Coincident γ rays
61	78, 86, 193, 266
78	266
86	61
135	200, 234, 370
151	279, 400
185	135, 234, 370
193	74
200	135, 151, 370
234	185
266	61, 78
279	135, 151
370	135, 185, 200, 637
400	151
637	370

obtained from the TAC spectrum between the ^{15}O particle and γ-ray signals. The decay curve for the 266-keV transition was analyzed by a convolution curve considering the time resolution of detectors; time spectrum of the 234-keV intraband transition of the $1/2^+$[620] band is shown as a typical time resolution of the detectors. Since the prompt part of the 193-keV time spectrum is contaminated with other γ rays with almost same energies ($5/2\ 3/2^+$[622] $\rightarrow$ $5/2\ 1/2^+$[620], $7/2\ 7/2^+$[613]), the lifetime was derived
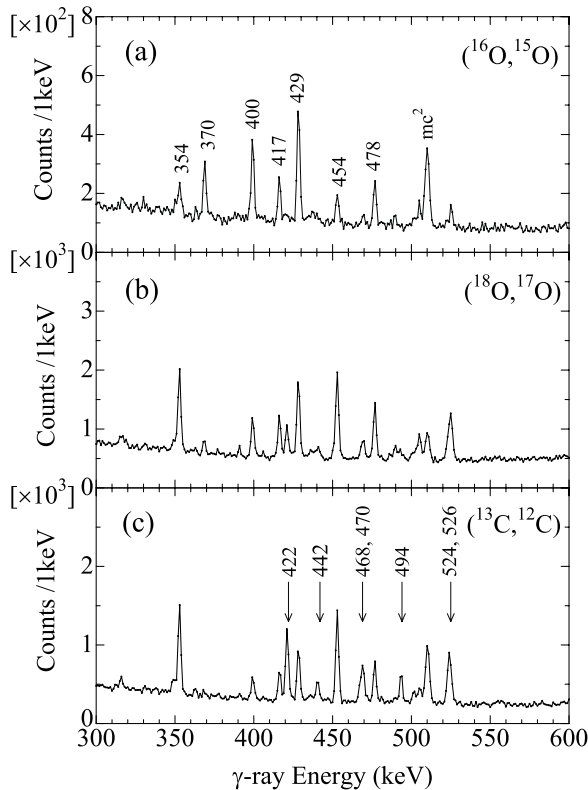
FIG. 4. Same as described in the caption to Fig. 3 but for 300 keV $< E_\gamma <$ 600 keV.
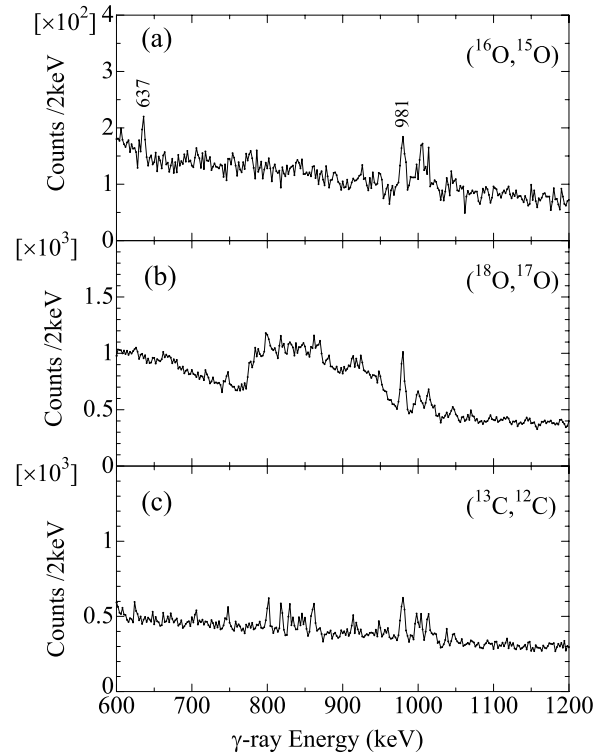
FIG. 5. Same as described in the caption to Fig. 3 but for 600 keV $< E_\gamma <$ 1200 keV.

from the data point apart from the prompt part, as shown by the fitting line in Fig. 9(b).

Figure 10 shows a 981-keV γ peak suffered by Doppler-shift, measured in the (^{18}O, ^{17}O) reaction. The 981-keV γ peak was shifted backward (forward) by the energy corresponding to the recoil speed of ^{249}Cm, when γ rays were measured by the combination of Ge detectors and adjacent (opposite) Si ΔE-E detectors placed in the reaction plane. Ge detectors placed out of the reaction plane observed γ rays at 90° with respect to the recoil direction. A ^{249}Cm nucleus recoils out at 66° with respect to the beam axis with initial velocity of $\beta = 0.0067$, when the ^{17}O particle is scattered at $-40°$. The 981-keV γ
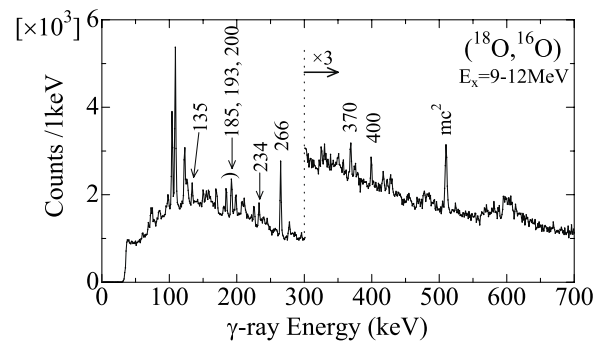
FIG. 6. γ-ray spectrum of ^{249}Cm measured in the (^{18}O,^{16}O) reaction. This spectrum was obtained by setting the gate on ^{16}O, whose kinetic energies correspond to the excitation of ^{250}Cm between 9 and 12 MeV. This excitation energy is high enough to evaporate one neutron, and thus γ rays in ^{249}Cm were observed.
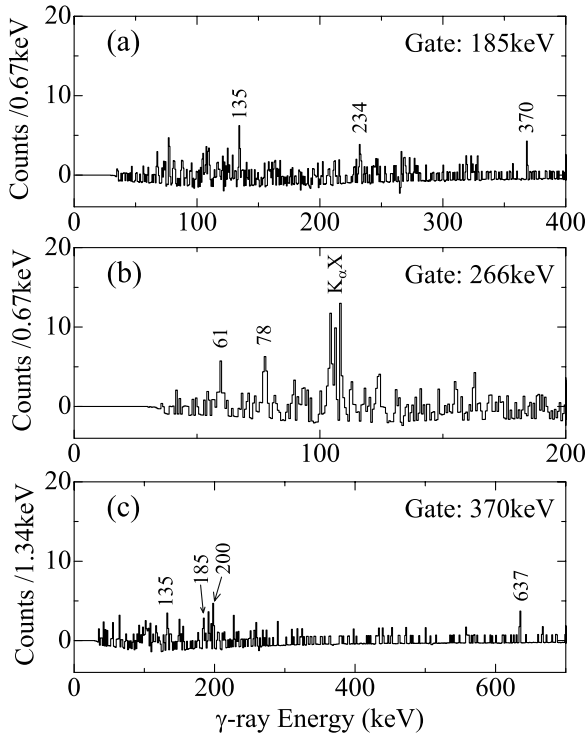
FIG. 7. γ-γ coincidence spectra of ^{249}Cm. These spectra were measured in the (^{16}O, ^{15}O) reaction and obtained by setting the gate on ^{15}O with $-1 < E_x < 5$ MeV. These spectra were in coincidence with (a) 185-keV (15/2 1/2$^+$[620] $\rightarrow$ 11/2 1/2$^+$[620]), (b) 266-keV (11/2 11/2$^-$[725] $\rightarrow$ 9/2 7/2$^+$[613]), and (c) 370-keV (19/2 1/2$^-$[750] $\rightarrow$ 17/2 1/2$^+$[620]) transitions.
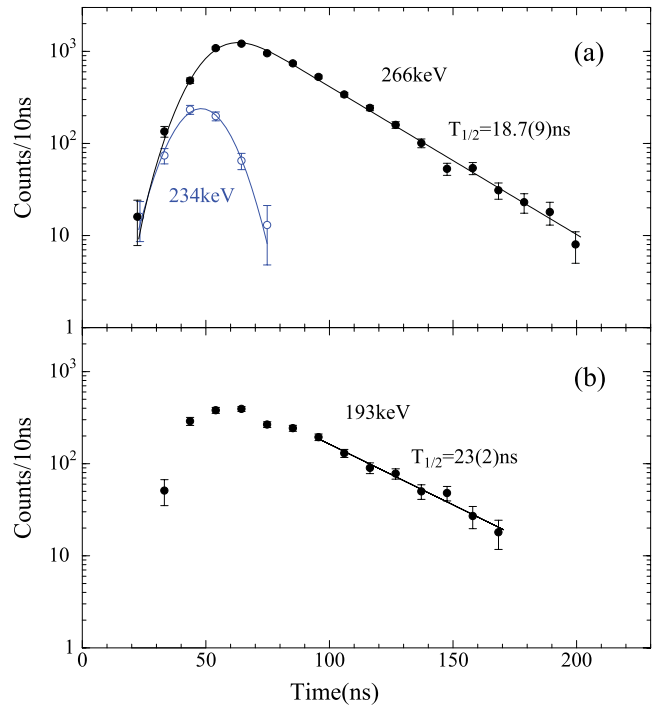

FIG. 9. (Color online) Decay curves for the 11/2 11/2$^-$[725] state at 375 keV. These time spectra were obtained from a TAC between particle signals of Si detectors and γ-ray signals of Ge detectors by setting the gate on ^{15}O in the (^{16}O, ^{15}O) reaction. (a) Time spectrum for the 266-keV transition. A prompt time spectrum for the 234-keV transition (19/2$^+$ $\rightarrow$ 15/2$^+$ in the 1/2$^+$[620] band) was also shown for comparison. (b) Time spectrum for the 193-keV transition.

peak shifted by about 5 keV, corresponding to the initial speed of ^{249}Cm. Because the target backing was thick enough to stop ^{249}Cm in it, observation of the fully Doppler-shifted γ peak

indicates that this γ ray is emitted before suffering the energy loss in the target. Therefore, the 981-keV γ ray is emitted from
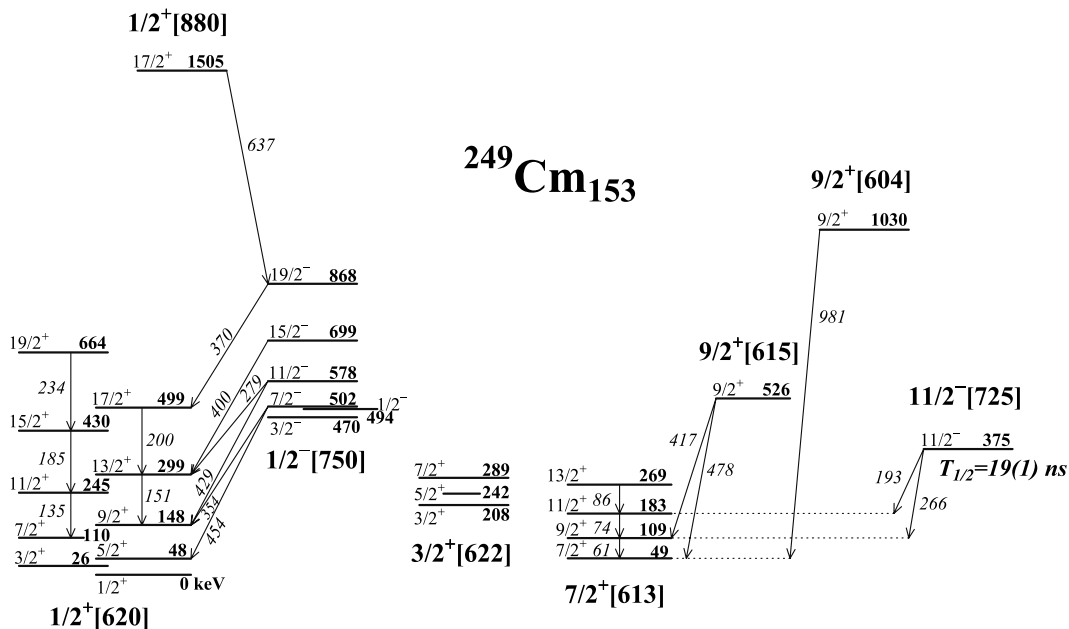

FIG. 8. Level scheme of ^{249}Cm. Energy levels identified in the present experiments are shown. γ rays observed in the (^{16}O, ^{15}O) reaction are depicted. The γ-ray and level energies are in units of keV.
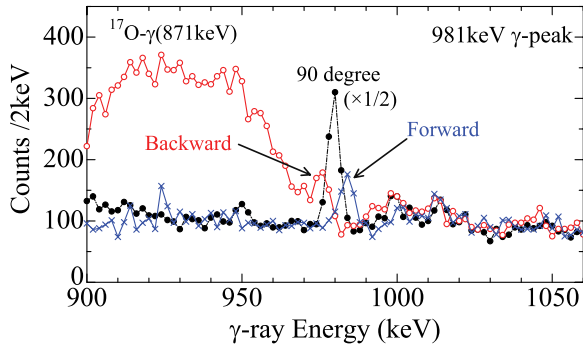
FIG. 10. (Color online) Doppler-shifted 981-keV γ peak measured in the $(^{18}O, ^{17}O)$ reaction. The 981-keV γ peak was shifted backward (forward) by the energy corresponding to the initial recoil speed of ^{249}Cm, when γ rays were measured by the combination of Ge detectors and adjacent (opposite) Si $\Delta E\text{-}E$ detectors placed in the reaction plane. Ge detectors placed out of the reaction plane observed γ rays at 90° with respect to the recoil direction. Because the target backing was thick enough to stop ^{249}Cm in it, observation of the fully Doppler-shifted γ peak indicates that this γ ray is emitted before suffering the energy loss in the target.

the state with a lifetime much shorter than the stopping time of 2 ps.

IV. DISCUSSION

A. Heavy-ion transfer reactions and γ-ray yields

Correlations between γ-ray yields and E_x, derived by the kinetic energies of outgoing particles, give a clue whether those γ rays are emitted from near the yrast line. Observed excited states are populated not only directly by the transfer reaction but also by successive decay from higher excited states. Because γ rays near the yrast line inherit higher excited states, γ-ray yields have a peak at a larger E_x. However, γ rays off the yrast line have E_x of the state populated by the direct reaction. Figures 11(a)–11(c) show γ-ray yields measured in the $(^{16}O, ^{15}O)$ reaction. γ rays near the yrast line have a peak around 3 MeV, whereas γ rays off the yrast line have a peak around 1 MeV. γ-ray yields in Fig. 11(d) were measured in the $(^{13}C, ^{12}C)$ reaction. Some γ-ray yields have a dip at about 3 MeV. This would be caused by the excitation of ^{12}C at 4.4 MeV by transfer of a neutron in the $p_{3/2}$ orbital of ^{13}C.

Figure 12 shows population yields of the members of the $1/2^-[750]$ band for the reactions of the $(^{16}O, ^{15}O)$, $(^{18}O, ^{17}O)$, and $(^{13}C, ^{12}C)$. The $1/2^-[750]$ band provides a good test of population yields. Because lower-spin members of this band are off the yrast line, they are mainly populated directly by the transfer reactions; this is valid at least $\leqslant 11/2^-$, as shown in the yield curve of the 429-keV transition in Fig. 11(b). Furthermore, the intraband transitions are weak, because inversion of spin sequence is not allowed to decay via $M1$ transitions. Therefore, the intensities of γ rays de-exciting the levels of this band can be used as population yields of those levels. As shown in Fig. 12, the $(^{16}O, ^{15}O)$ reaction populates higher-spin members (the maximum yield is at 11/2), although the yields for lower-spin states are much smaller than those

by the other reactions. This is caused by matching condition of angular momentum. Ground-state to ground-state Q values, Q_{gg}, for the $(^{16}O, ^{15}O)$, $(^{18}O, ^{17}O)$, and $(^{13}C, ^{12}C)$ reactions are -11.0, -3.3, and -0.2 MeV, respectively. The highly negative Q_{gg} value of the $(^{16}O, ^{15}O)$ reaction suppresses the population of low-j orbitals and enhances that of high-j orbitals.

B. $1/2^+[620]$ band

The energy levels up to $9/2^+$ of the $1/2^+[620]$ band were identified by the (d, p) transfer reaction [15] and the levels up to $7/2^+$ were measured by the (n, γ) experiment [16]. We extended up to $19/2^+$. We have found the γ-γ correlations for the cascades of 234–185–135 keV and 200–151 keV transitions. Furthermore, the coincidences of the 200–135, 279–135, and 370–185–135 keV transitions were observed, indicating that the transitions between the $13/2^+$ and $11/2^+$ states and between the $17/2^+$ and $15/2^+$ states have significant transition strength by internal conversion electrons. In-plane to out-of-plane γ-ray anisotropies suggest that the 234–185–135 and 200–151 keV transitions are stretched $E2$ types. As shown in Fig. 11(a), the yield curves for the 234- and 185-keV γ rays have a peak at E_x over 3 MeV, which is consistent with these states being near the yrast line.

Using the energies of levels up to $19/2^+$, rotational parameter $A(= \hbar^2/2\mathcal{I})$ and decoupling parameter a were derived as $A = 6.4$ keV and $a = 0.37$, close to the calculated value of $a = 0.40$ [3]. The calculation using the $M1$ matrix elements [2] shows that the $B(M1; 17/2^+ \rightarrow 15/2^+)$ and $B(M1; 15/2^+ \rightarrow 13/2^+)$ values are 0.46 and 0.032 μ_N^2, respectively. Therefore, the former transition is stronger than that the latter in spite of their transition energies. This is consistent with the fact that the $17/2^+$ state decays to the $15/2^+$ state, whereas the $M1$ transition between the $15/2^+$ and $13/2^+$ states was not observed.

C. $1/2^-[750]$ band

The $3/2^-, 7/2^-$, and $11/2^-$ states of the $1/2^-[750]$ band were identified by the (d, p) transfer reaction [15] and the $3/2^-$ and $1/2^-$ states were observed by the (n, γ) experiment [16]. Although the 546.86-keV level was assigned to the 5/2 member [16], we did not adopt this assignment. This is because this level does not decay to states of the $1/2^+[620]$ band but to those of the $3/2^+[622]$ band, which is very different from other $1/2^-[750]$ members decaying to states of the $1/2^+[620]$ band. We extended up to $19/2^-$ in the present study. In-plane to out-of-plane γ-ray anisotropies suggest that interband transitions between $1/2^-[750]$ and $1/2^+[620]$ are $E1$ types. The observed members except for $19/2^-$ can be populated directly in the transfer reactions; the $19/2^-$ state could not be populated directly, because this state hardly contains the spherical single-particle component of $l_{19/2}$. The observation of the 400- and 370-keV γ-rays in the $(^{18}O, ^{16}O)$ reaction, shown in Fig. 6, indicates that the $15/2^-$ and $19/2^-$ states can be populated from higher excited states.

Using the energies of the $3/2^-, 7/2^-, 11/2^-, 15/2^-$, and $19/2^-$ levels, we obtained as $A = 5.6$ keV and $a = -3.2$,
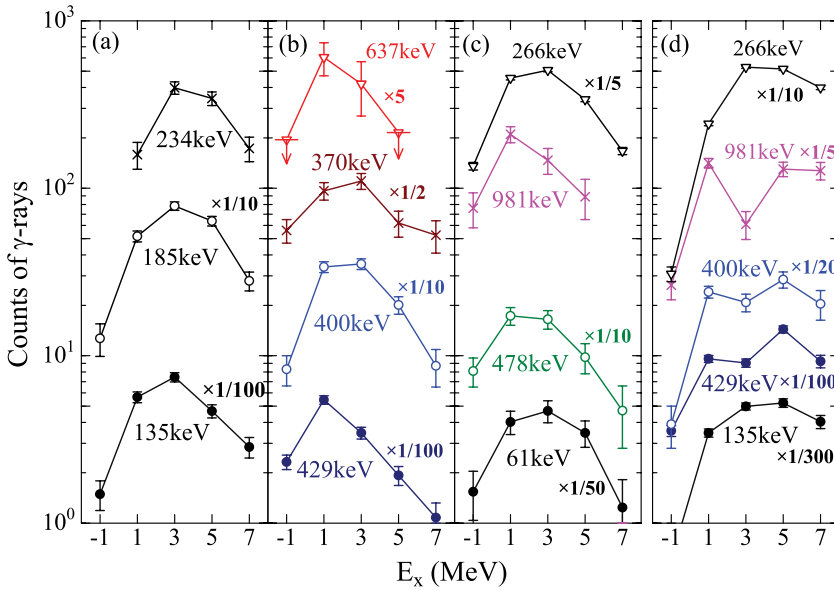
FIG. 11. (Color online) γ-ray yields against excitation energies of ^{249}Cm. γ-ray yields measured in the (^{16}O, ^{15}O) reaction are shown in (a), (b), and (c) for some γ rays. In (d), γ-ray yields measured in the (^{13}C, ^{12}C) reaction are shown. Excitation energies E_x of ^{249}Cm were derived from the kinetic energies of outgoing particles. Note that E_x has a poor resolution of abut 2 MeV.

close to the calculated value of $a = -3.8$ [3]. Because this decoupling parameter induces the inversion of spin sequence, the states of this band cannot be connected by $M1$ transitions. Branching ratios of $E1$ transitions are explained by calculation using $E1$ matrix elements [2], e.g., the $B(E1; 11/2^- \rightarrow 13/2^+)/B(E1; 11/2^- \rightarrow 9/2^+)$ and $B(E1; 11/2^- \rightarrow 11/2^+)/B(E1; 11/2^- \rightarrow 9/2^+)$ ratios were obtained as 1.3(2) and $<5 \times 10^{-2}$, respectively, which

are consistent with the calculated values of 2.1 and 9.1×10^{-3}, respectively.

D. $1/2^+$[880] band

Energy levels at 1560 or 1898 keV in ^{249}Cm were tentatively assigned to the $17/2^+$ state of the $1/2^+$[880] band by the (^{4}He,^{3}He) stripping reaction experiment [4]. We have assigned the 1505-keV level to the $17/2$ $1/2^+$[880] state by the present experiment. The 1505-keV level would be identical to the 1560-keV level observed by the (^{4}He, ^{3}He) experiment, in which ^{3}He had a energy resolution of 45 keV.

In the present experiment, the 637-keV γ ray was found to be coincident with the 370-keV transition de-exciting the $19/2^-$ state of the $1/2^-$[750] band, shown in Fig. 7(c). The 637-keV transition was only observed by the (^{16}O, ^{15}O) reaction and neither by the (^{13}C, ^{12}C) nor by the (^{18}O, ^{17}O) reaction. This fact suggests that the 637-keV transition de-excites a state with a high-j orbital. The most probable state at 1505 keV is the $17/2^+$ state of the $1/2^+$[880] band. The γ-ray yield vs. E_x for the 637-keV transition, shown in Fig. 11(b), has a maximum yield at about 1.5 MeV. This result is consistent with the 1505-keV level being off the yrast line and being directly populated by the transfer reaction.

The assignment of the $17/2$ $1/2^+$[880] state to the 1505-keV level is also supported by the following consideration. The $17/2^+$ state has the largest cross section among the members of the $1/2^+$[880] band, and the $13/2^+$ state has the next, because spherical single particle components C_j^2 are 0.74 and 0.21 for the $17/2^+$ and $13/2^+$ states, respectively [4]. Furthermore, the intraband transitions from the $17/2^+$ state to other members in lower energy must be weak, because spin sequence of the $1/2^+$[880] band would be very different from usual bands owing to a large decoupling parameter (a calculated value of $a = 8.3$ [4]); $9/2^+$, $5/2^+$, $13/2^+$, $1/2^+$, and $17/2^+$ levels are calculated to be 1368, 1372, 1412, 1423, and 1505 keV, using this decoupling parameter and $A = 6.0$ keV. Therefore, it is reasonable that the $17/2^+$ state is directly populated by the
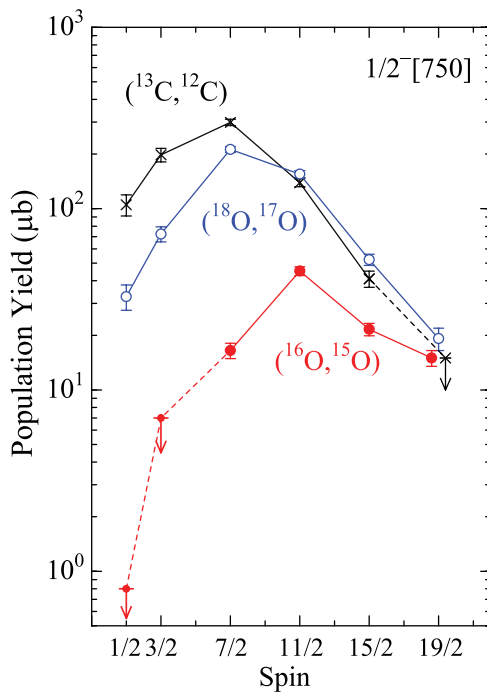

FIG. 12. (Color online) Population yields of members of the $1/2^-$[750] band for different heavy-ion transfer reactions. The yields were obtained from the intensities of γ rays de-exciting the states of the $1/2^-$[750] band. The (^{16}O, ^{15}O), (^{18}O, ^{17}O), and (^{13}C, ^{12}C) reactions have $Q_{gg} = -11.0$, -3.3, and -0.2 MeV, respectively.

transfer reaction and decays through an $E1$ transition to a state with the same K number.

The reason why the transition between the $17/2^+$ state and the $15/2^-$ state at 699 keV was not observed can be also explained. The $B(E1)$ values are calculated as:

$$B(E1; 17/2^+ \rightarrow 19/2^-) = \tfrac{5}{19}C \times [\sqrt{2}G_{E1} + G'_{E1}]^2, \quad (1)$$

$$B(E1; 17/2^+ \rightarrow 15/2^-) = \tfrac{4}{17}C \times [-\sqrt{2}G_{E1} + G'_{E1}]^2, \quad (2)$$

where C is a constant of 0.50 e^2fm^2 for ^{249}Cm, and G_{E1} and G'_{E1} are $E1$ matrix elements for $K = 1/2 \rightarrow K' = 1/2$ and $K = 1/2 \rightarrow K' = -1/2$, respectively, between $1/2^+[880]$ and $1/2^-[750]$. Using $G'_{E1}/G_{E1} = 0.50$ [2,28], the $B(E1; 17/2^+ \rightarrow 15/2^-)/B(E1; 17/2^+ \rightarrow 19/2^-)$ ratio is obtained to be 0.20, then the γ-ray intensity ratio, $I_\gamma(17/2^+ \rightarrow 15/2^-)/I_\gamma(17/2^+ \rightarrow 19/2^-)$, is 0.41. In Eq. (2), matrix elements of G_{E1} and G'_{E1} cancel each other. Therefore, a small modification of these matrix elements would result in a much smaller $B(E1; 17/2^+ \rightarrow 15/2^-)$ value.

The single-particle energy of $1/2^+[880]$ was calculated by Chasman using a momentum-dependent Woods-Saxon potential and a momentum-independent Woods-Saxon potential [3,29]. The experimental result supports the former potential; the former and the latter give the bandhead energies of the $1/2^+[880]$ band as 1.4 and 2.0 MeV, respectively. We expect development of theoretical approaches to calculating an accurate quasiparticle energy of $1/2^+[880]$ by a self-consistent theory, such as a relativistic mean-field theory [30], to predict the structure of superheavy nuclei.

E. 3/2$^+$[622] band

The $3/2^+$, $5/2^+$, $7/2^+$, and $9/2^+$ states of the $3/2^+[622]$ band were identified by the (d, p) transfer reaction [15] and the $3/2^+$, $5/2^+$, and $7/2^+$ states were observed by the (n, γ) experiment [16]. The transitions de-exciting the states of this band were observed in the $(^{13}C, {}^{12}C)$ reaction, as shown in Fig. 3(c); the γ peaks of these transitions were overlapped each other, because the states of this band decay both to those of $1/2^+[620]$ and $7/2^+[613]$ bands having states close in energy (e.g., $5/2$ $1/2^+[620]$ and $7/2$ $7/2^+[613]$ states lie at 48.20 and 48.74 keV, respectively [16]). However, those transitions de-exciting the $3/2^+[622]$ states were observed very weakly in the $(^{16}O, {}^{15}O)$ reaction, consistent with the properties of this reaction that population of low-j orbitals are suppressed.

F. 7/2$^+$[613] band

The $7/2^+$ and $9/2^+$ states of the $7/2^+[613]$ band were measured by the α decay of ^{253}Cf [14], and the lifetime of the $7/2^+$ state was cited as $T_{1/2} = 23 \, \mu$s [31]. The $9/2^+$ level was assigned by the (d, p) transfer reaction [15] and the $7/2^+$ state was measured by the (n, γ) experiment [16]. We have extended up to $13/2^+$ states. These states are connected by $M1$ cascades. In-plane to out-of-plane γ-ray anisotropies suggest that the 61-, 74-, and 86-keV transitions are $M1$ types.

G. 9/2$^+$[615] band

Energy levels at 220 and 300 keV in ^{249}Cm were assigned to the $9/2^+$ and $11/2^+$ states of the $9/2^+[615]$ band, respectively, by the (d, p) transfer reaction with a "plausible" confidence level [15]. However, those states in ^{251}Cf were observed clearly at 683 and 758 keV by the (d, p) transfer reaction [3]. Other quasiparticle states of ^{249}Cm are close in energy to those of ^{251}Cf with energy differences of $\lesssim$100 keV. It is not plausible that only the $9/2^+[615]$ quasiparticle state is different from that of ^{251}Cf by over 400 keV.

We have assigned the 526-keV level to the $9/2$ $9/2^+[615]$ state. In the present work, the 477.6- and 417.0-keV transitions were observed. Because the energy difference of 60.6(1) keV between these two transitions accord with the energy difference of 60.8(1) keV between the $9/2^+$ and $7/2^+$ states of the $7/2^+[613]$ band, we have established the 526-keV level decaying to these $7/2^+[613]$ states. The γ-ray anisotropy data of the 478- and 417-keV transitions suggest that this level has spin $9/2^+$. Furthermore, the γ-ray yield vs. E_x for the 478 keV transition, shown in Fig. 11(c), is consistent with this level being populated directly by the transfer reaction. The 528(3)-keV level observed by the (d, p) experiment [15] would correspond to this level.

The $M1$ matrix elements between $9/2^+[615]$ and $7/2^+[613]$ states are very small. Using $G_{M1} = 0.038$ [2], we obtained as $B(M1; 9/2^+ \rightarrow 7/2^+) = 2.6 \times 10^{-4} \, \mu_N^2$, corresponding to the partial halflife of 1.4 ns. Therefore, the 417- and 478-keV transitions should have a significant mixing of $E2$. Assuming a mixing ratio of $\delta \sim 0.1$ for these transitions, the in-plane to out-of-plane anisotropies obtained in the experiment can be explained.

H. 9/2$^+$[604] band

We have established the $9/2$ $9/2^+[604]$ state at 1030 keV. In the present experiment, we have found a strong γ ray of 981 keV. The γ-ray yield vs. E_x, shown in Fig. 11(c), shows that this transition de-excites the state off the yrast line. Furthermore, the 981-keV transition was found to have a very short lifetime of $T_{1/2} \ll 2$ ps, shown in Fig. 10. In the (d, p) reaction, a strongly populated level at 1030 keV was observed [15]. Therefore, we placed the 981-keV transition on the $7/2$ $7/2^+[613]$ state at 49 keV, leading to the 1030-keV level. In ^{251}Cf, the 974-keV level was assigned to the $9/2$ $9/2^+[604]$ state [12]; this level was also strongly populated by the ^{250}Cf(d, p) transfer reaction [3].

The $9/2^+[604]$ and $7/2^+[613]$ states are connected by an allowed $M1$ transition ($\Delta n_z = +1$, and $\Delta \Lambda = -1$ [32]). Using $G_{M1} = -1.73$ [2], we calculated the $B(M1; 9/2^+ \rightarrow 7/2^+)$ value as 0.57 μ_N^2, corresponding to $T_{1/2} = 0.07$ ps. The experimental result of the lifetime of the 981-keV transition agrees with this assignment.

I. 11/2$^-$[725] band

We have established the $11/2$ $11/2^-[725]$ state at 375 keV. This state has a half-life of 19(1) ns, and decays to the $11/2^+$ and $9/2^+$ states of the $7/2^+[613]$ band through the 193- and

266-keV transitions, respectively. The γ-γ coincidence data, shown in Fig. 7(b) and Table II, support this assignment. In-plane to out-of-plane γ-ray anisotropies vanish because of the long lifetime of this state. The 193- and 266-keV γ transitions were observed strongly in the (^{18}O,^{16}O) reaction as shown in Fig. 6, because the 11/2 $11/2^-$[725] state lies near the yrast line.

The transitions between the $11/2^-$[725] and $7/2^+$[613] states are forbidden because of $\Delta K = 2$. Therefore, it is reasonable that the $11/2^-$ state has a long lifetime. Although the $9/2^-$[734] quasiparticle state lying below the Fermi level was not observed in the present stripping reaction, this band should lie close in energy to the $11/2^-$[725] band. In ^{251}Cf, the 11/2 $11/2^-$[725] and 9/2 $9/2^-$[734] states are at 370 and 434 keV, respectively. Because the $11/2^-$[725] and $9/2^-$[734] orbitals originate from the $j_{15/2}$ unique parity state, these bands have strong Coriolis mixing. As a result, the level spacings of the $11/2^-$[725] band would be much smaller than those of other usual bands; a rotational parameter of $A < 5$ keV is possible on a reasonable assumption.

The transfer reaction populates the 15/2 member, because the $11/2^-$[725] quasiparticle state has a major component of the $j_{15/2}$ spherical single-particle state. In the present work, the γ-rays de-exciting the $15/2^-$ state could not be identified. This was probably because level spacings would be small, and thus γ rays do not have enough intensity to be observed due to large internal conversions. The 78-keV transition was found to be coincident with the 266-keV transition. However, it is not sure that this transition is an intraband transition of the $11/2^-$[725] band, because the other cascade transition from the $15/2^-$ state was not observed.

V. CONCLUSION

Quasiparticle states in ^{249}Cm$_{153}$ were investigated by in-beam γ-ray spectroscopy using heavy-ion transfer reactions. Reaction channels and excitation energies of ^{249}Cm were selected by measuring kinetic energies of outgoing particles using Si ΔE-E detectors placed around the grazing angle. It was demonstrated that high-j orbitals in ^{249}Cm were populated by the (^{16}O, ^{15}O) reaction having a large negative Q value. The observed level structure of ^{249}Cm is similar to that of ^{251}Cf with the same neutron number. We have established the 17/2 $1/2^+$[880] state, originating from the $k_{17/2}$ spherical single-particle state, at 1505 keV in ^{249}Cm. This low excitation energy agrees with the calculation using a momentum-dependent Woods-Saxon potential. The calculation of the quasiparticle energy of $1/2^+$[880] is sensitive to theoretical models and parameters employed in it. Further theoretical studies by different approaches are required to give an accurate prediction of structure of super-heavy nuclei.

[1] I. Ahmad, A. M. Friedman, R. R. Chasman, and S. W. Yates, Phys. Rev. Lett. **39**, 12 (1977).

[2] R. R. Chasman, I. Ahmad, A. M. Friedman, and J. R. Erskine, Rev. Mod. Phys. **49**, 833 (1977).

[3] I. Ahmad, R. R. Chasman, A. M. Friedman, and S. W. Yates, Phys. Lett. **B251**, 338 (1990).

[4] I. Ahmad, B. B. Back, R. R. Chasman, J. P. Greene, T. Ishii, L. R. Morss, G. P. A. Berg, A. D. Bacher, C. C. Foster, W. R. Lozowski *et al.*, Nucl. Phys. **A646**, 175 (1999).

[5] R.-D. Herzberg, J. Phys. G **30**, R123 (2004).

[6] R.-D. Herzberg, P. T. Greenlees, P. A. Butler, G. D. Jones, M. Venhart, I. G. Darby, S. Eeckhaudt, K. Eskola, T. Grahn, C. Gray-Jones *et al.*, Nature (London) **442**, 896 (2006).

[7] P. Reiter, T. L. Khoo, I. Ahmad, A. V. Afanasjev, A. Heinz, T. Lauritsen, C. J. Lister, D. Seweryniak, P. Bhattacharyya, P. A. Butler *et al.*, Phys. Rev. Lett. **95**, 032501 (2005).

[8] S. K. Tandel, T. L. Khoo, D. Seweryniak, G. Mukherjee, I. Ahmad, B. Back, R. Blinstrup, M. P. Carpenter, J. Chapman, P. Chowdhury *et al.*, Phys. Rev. Lett. **97**, 082502 (2006).

[9] M. Asai, K. Tsukada, M. Sakama, S. Ichikawa, T. Ishii, Y. Nagame, I. Nishinaka, K. Akiyama, A. Osa, Y. Oura *et al.*, Phys. Rev. Lett. **95**, 102502 (2005).

[10] I. Ahmad, F. T. Porter, M. S. Freedman, R. F. Barnes, R. K. Sjoblom, F. Wagner, J. Milsted, and P. R. Fields, Phys. Rev. C **3**, 390 (1971).

[11] I. Ahmad and J. Milsted, Nucl. Phys. **A239**, 1 (1975).

[12] I. Ahmad, M. P. Carpenter, R. R. Chasman, J. P. Greene, R. V. F. Janssens, T. L. Khoo, F. G. Kondev, T. Lauritsen, C. J. Lister, P. Reiter *et al.*, Phys. Rev. C **62**, 064302 (2000).

[13] I. Ahmad, J. P. Greene, E. F. Moore, F. G. Kondev, R. R. Chasman, C. E. Porter, and L. K. Felker, Phys. Rev. C **72**, 054308 (2005).

[14] C. E. Bemis and J. Halperin, Nucl. Phys. **A121**, 433 (1968).

[15] T. H. Braid, R. R. Chasman, J. R. Erskine, and A. M. Friedman, Phys. Rev. C **4**, 247 (1971).

[16] R. W. Hoff, W. F. Davidson, D. D. Warner, H. G. Börner, and T. von Egidy, Phys. Rev. C **25**, 2232 (1982).

[17] T. Ishii, S. Shigematsu, M. Asai, A. Makishima, M. Matsuda, J. Kaneko, I. Hossain, S. Ichikawa, T. Kohno, and M. Ogawa, Phys. Rev. C **72**, 021301(R) (2005).

[18] T. Ishii, S. Shigematsu, H. Makii, M. Asai, K. Tsukada, A. Toyoshima, M. Matsuda, A. Makishima, T. Shizuma, J. Kaneko *et al.*, J. Phys. Soc. Jpn. **75**, 043201 (2006).

[19] T. Ishii, H. Makii, M. Asai, S. Shigamatsu, K. Tsukada, A. Toyoshima, M. Matsuda, A. Makishima, J. Kaneko, H. Toume *et al.*, Phys. Rev. C **76**, 011303(R) (2007).

[20] H. Makii, T. Ishii, M. Asai, K. Tsukada, A. Toyoshima, M. Matsuda, A. Makishima, J. Kaneko, H. Toume, S. Ichikawa *et al.*, Phys. Rev. C **76**, 061301(R) (2007).

[21] P. D. Bond, J. Barrette, C. Baktash, C. E. Thorn, and A. J. Kreiner, Phys. Rev. Lett. **46**, 1565 (1981).

[22] M. Sataka, S. Takeuchi, Y. Tsukihashi, K. Horie, I. Ouchi, S. Hanashima, S. Abe, N. Ishizaki, H. Tayama, A. Osa *et al.*, in *JAEA-Tokai TANDEM Annual Report 2006*, edited by T. Ishii, Y. Nagame, S. Chiba, N. Ishikawa, Y. Toh, A. Osa, and M. Sataka

(Japan Atomic Energy Agency, 2008), JAEA-Review 2007-046, pp. 3–5.

[23] R. Bass, *Nuclear Reactions with Heavy Ions* (Springer-Verlag, New York, 1980).

[24] M. H. Macfarlane and S. C. Pieper, technical report, ANL-76-11, 1978.

[25] F. Rösel, H. M. Fries, K. Alder, and H. C. Pauli, At. Data Nucl. Data Tables **21**, 291 (1978).

[26] B. B. Back, O. Hansen, H. C. Britt, and J. D. Garrett, Phys. Rev. C **9**, 1924 (1974).

[27] S. R. de Groot, H. A. Tolhoek, and W. J. Huiskamp, in *Alpha-, Beta- and Gamma-ray Spectroscopy*, edited by K. Siegbahn (North-Holland, Amsterdam, 1965), Vol. 2, pp. 1199–1261.

[28] R. R. Chasman and I. Ahmad (private communication).

[29] R. R. Chasman and I. Ahmad, Phys. Lett. **B392**, 255 (1997).

[30] A. V. Afanasjev, T. L. Khoo, S. Frauendorf, G. A. Lalazissis, and I. Ahmad, Phys. Rev. C **67**, 024309 (2003).

[31] A. Artna-Cohen, Nucl. Data Sheets **88**, 155 (1999).

[32] G. Alaga, Nucl. Phys. **4**, 625 (1957).